Indian Geotechnical Journal, 33 (4), 2003

Response of Extensible Reinforcement to Transverse Pull/Displacement: Linear Subgrade Behavior

M.R. Madhav* and B. Umashankar†

Introduction

Reinforced soil technique is adopted to a wide variety of applications such as reinforced soil walls, reinforced soil slopes, and reinforced embankments constructed over soft or unstable foundation, etc. The reinforcement in all the above instances is in the form of strips, bars, grids or sheets fabricated or manufactured from metal or geosynthetics. The reinforcement restrains tensile strains in the soil and thus increases the over all resistance of the composite medium through interfacial bond resistance but limited by its own tensile strength. The bond resistance that operates in reinforced soil is determined either by direct shear or axial pull out tests (Jewell, 1996). Considerable literature is available (McGown et al., 1982; Ingold, 1983; Jewell at al., 1984; Juran et al., 1988; Farrag et al., 1993; Hayashi et al., 1994; Alfaro et al., 1995; Lopes and Ladeira, 1996; Ochiai et al., 1996; Sobhi and Wu, 1996; etc.) on the test procedures, analysis and interpretation of axial pull out tests.

However, the kinematics of failure (Fig.1) is usually such that the failure surface intersects the reinforcement obliquely. The reinforcement is thus subjected to both axial and transverse components of the force by the sliding mass of soil. Most available theories for the analysis and design of reinforced soil structures consider only the axial resistance of the reinforcement to pullout (Fowler, 1982 and Jewell, 1996) and not the

* Professor, Department of Civil Engineering, Indian Institute of Technology, Kanpur – 208016, UP, India. E-mail: madhav@iitk.ac.in

† Graduate Student, Department of Civil Engineering, Indian Institute of Technology, Kanpur – 208016, UP, India. E-mail: umavijji@yahoo.com

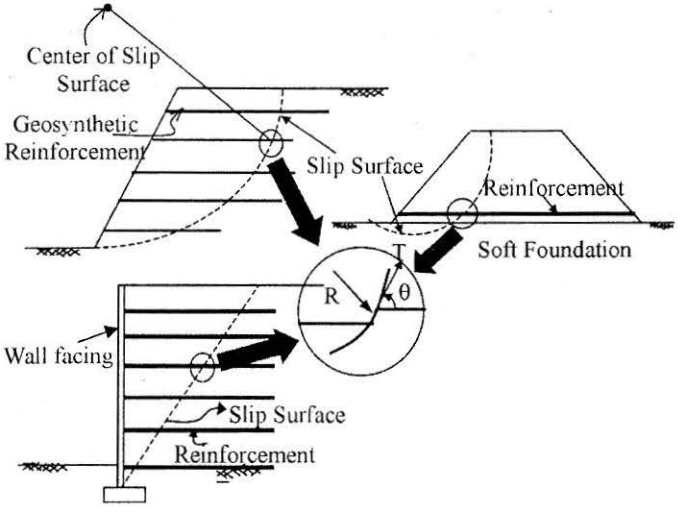

FIGURE 1 : Kinematics of Reinforced Slopes, Embankments and Retaining Walls

transverse one. The reinforcement force (Fig.2) is considered to act tangentially by Quast (1983) and Delmas et al. (1992) or along a direction between reinforcement and the tangent to the slip surface (Rowe, 1984; Low and Duncan, 1985; Bonaparte, 1987; Huisman, 1987; Leshchinsky and Boedeker, 1989; Rowe, 1992; Bergado and Long, 1997). Under the action of axial pull, the normal stresses on the reinforcement-soil interface remain the same as the gravity stresses. Consequently, the shear resistance mobilized at the interface is proportional to only these normal stresses. However, under the action of transverse force or displacement, the soil beneath the reinforcement mobilizes additional normal stresses as the reinforcement

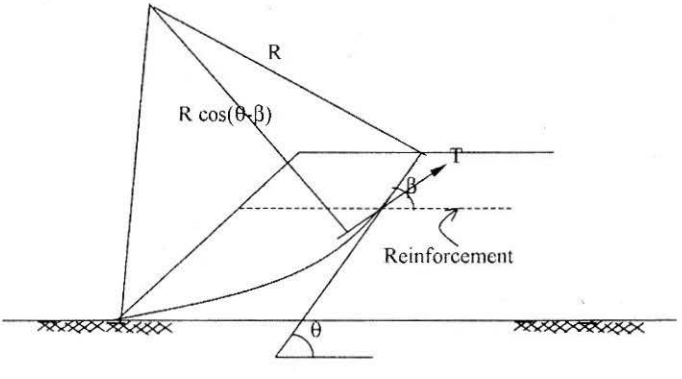

FIGURE 2 : Oblique Force in the Reinforcement (Bergado and Long, 1997)

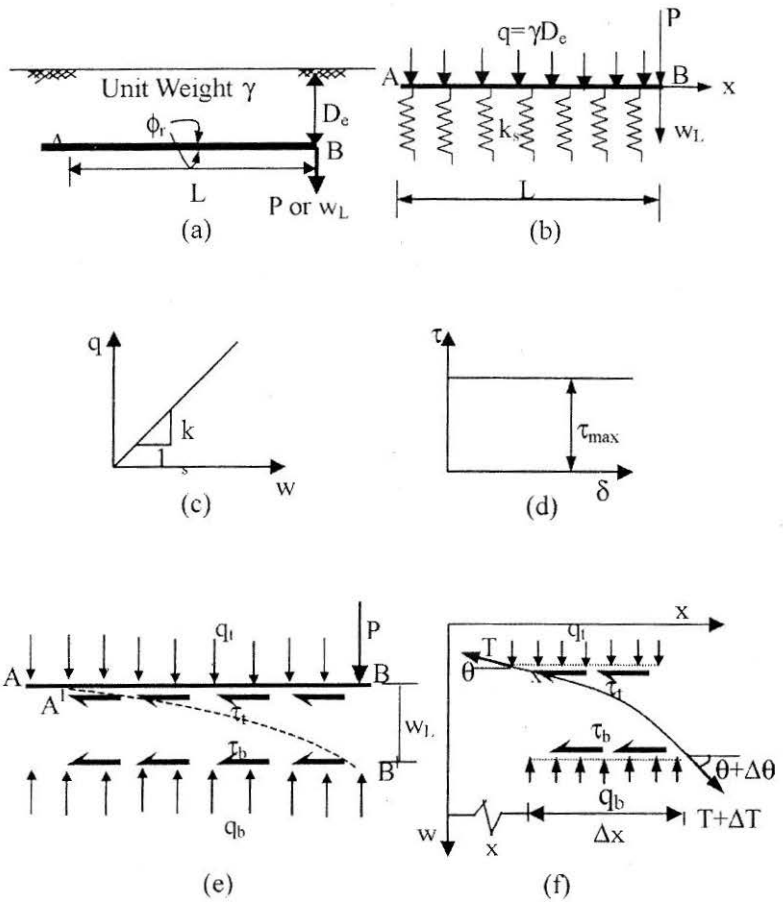

FIGURE 3 : Definition Sketch (a) Reinforcement Subjected to Transverse Force, (b) Model (c) Normal Stress-Displacement Response of Fill/Subgrade (d) Shear Stress- Horizontal Displacement Response of Interface (e) Deformed Profile and (f) Forces on an Element

deforms transversely. As a result, the shear resistance mobilized could be considerably different in case of reinforcement subjected to transverse force. Madhav and Umashankar (2002) studied the response of sheet reinforcement to transverse pull/displacement considering linear subgrade and inextensible reinforcement. In this paper, a method is presented for the estimation of the pull out resistance of sheet reinforcement subjected to transverse force assuming linear responses of the ground and extensible reinforcement.

Problem Definition and Analysis

Figure 3a depicts an extensible sheet reinforcement of length, L,

embedded at depth, D_e, from the surface, in a soil with a unit weight, γ, and subjected to a transverse force, P, at one of its extremes. The interface angle of shearing resistance between the reinforcement and the soil is ϕ_r. The response of the reinforcement to the transverse force is to be obtained in terms of a relation between the force, P, and the normal displacement, w_L, at point B. The model proposed for the analysis is shown in Fig.3b. The reinforcement and the underlying soil responses are represented respectively by a rough membrane and a set of Winkler springs. The fill/subgrade response is linear (Fig.3c) while the rigid plastic resistance of the interface is depicted in Fig.3d. Figure 3e represents the deformed profile of the reinforcement. Even though the reinforcement is extensible, it is possible a portion A-A^1 of the reinforcement remains unstretched without undergoing any extension whereas the portion of the reinforcement between A^1 and B undergoes transverse as well as horizontal displacements under the application of transverse displacement/force at point B. Thus shear stresses are mobilized only in the stretch A^1-B of the reinforcement. No tension is mobilized at and to the left of point A^1. The length 'A^{1}B' over which the shear stresses are mobilized is defined as the "active length of reinforcement", x_o. q_t and q_b and τ_t and τ_b are the normal and shear stresses acting on the top and the bottom surfaces respectively of the reinforcement over the portion A^{1}B . The normal stress-displacement relation of the soil is characterised by the relation

$$q = k_s w \tag{1}$$

where k_s = modulus of subgrade reaction (Terzaghi 1955), and

w = the transverse displacement

Considering an infinitesimal element (Fig.3f) of length, Δx, unit width, the tensions and their inclinations with the horizontal at distances x and $x + \Delta x$, are T and $(T + \Delta T)$ and θ and $(\theta + \Delta\theta)$ respectively. The horizontal and vertical force equilibrium relations for the element are

$$(T+\Delta T)\cos(\theta+\Delta\theta) - T\cos\theta - (q_t + q_b)\tan\phi_r \cdot \Delta x = 0 \tag{2}$$

and

$$(T+\Delta T)\sin(\theta+\Delta\theta) - T\cos\theta - (q_t + q_b)\tan\phi_r \cdot \Delta x = 0 \tag{3}$$

Equations (2) and (3) on simplification reduce to

$$\cos\theta\frac{dT}{dx} - T\sin\theta\frac{d\theta}{dx} - (q_t + q_b)\tan\phi_r = 0 \tag{4}$$

and

$$\sin\theta\frac{dT}{dx}-T\cos\theta\frac{d\theta}{dx}-(q_b-q_t)\;=\;0 \tag{5}$$

Multiplying Eqn.(4) with $\cos\theta$ and Eqn.(5) with $\sin\theta$ and adding the two, one gets

$$\frac{dT}{dx}\;=\;(q_t+q_b)\cos\theta\cdot\tan\phi_r+(q_b-q_t)\sin\theta \tag{6}$$

Similarly, multiplying Eqn.(4) by $\sin\theta$ and Eqn.(5) by $\cos\theta$ and subtracting the latter from the former, one gets

$$-T\frac{d\theta}{dx}-(q_t+q_b)\tan\phi_r\sin\theta+(q_b-q_t)\cos\theta\;=\;0 \tag{7}$$

But $\tan\theta=dw/dx$ and $d\theta/dx=\cos^2\theta\left(d^2w/dx^2\right)$ and the subgrade (Winkler spring) response to the increase in normal stress, (q_b-q_t) is equal to $k_s\cdot w$. Substituting for these in Eqns.(6) and (7) and simplifying for small values of θ (i.e. $\cos\theta=1$, $\sin\theta=\theta=0$), the coupled governing equations for the reinforcement subjected to transverse force are

$$\frac{dT}{dx}\;=\;(q_t+q_b)\tan\phi_r\;=\;(k_s w+2\gamma D_e)\tan\phi_r \tag{8}$$

and

$$-T\frac{d^2w}{dx^2}+k_s\cdot w\;=\;0 \tag{9}$$

The original problem is to derive the response of the reinforcement in terms of w and T for a given applied transverse force, P. However, it was found simpler to obtain the force, P, for a given free end displacement, w_L.

The boundary conditions are: at x = 0, the slope, dw/dx, of and tension in the reinforcement, T, are zero, and at x = L, the displacement $w = w_L$.

The applied transverse load, P, is obtained from the vertical equilibrium of forces as

$$P\;=\;\int_0^L K_s\cdot w\cdot dx \tag{10}$$

Non-dimensionalising Eqns.(8), (9) and (10) with $X = x/L$, $W = w/w_L$, $T^* = T/T_{max\,ap}$ where $T_{max\,ap} = 2\gamma D_e L \tan\phi_r$, the axial pullout capacity, and $P^* = P/\gamma D_e L$, one gets

$$\frac{dT^*}{dX} = \frac{\{\mu W_L W + 2\}}{2} \tag{11}$$

$$-T^* \frac{d^2W}{dX^2} + \frac{\mu W}{(2\tan\phi_r)} = 0 \tag{12}$$

and

$$P^* = \mu W_L \int_0^1 W \cdot dX \tag{13}$$

where $\mu = k_s L/\gamma D_e$, a relative subgrade stiffness factor, and

$W_L = w_L/L$

The boundary conditions become: at X = 0, $T^* = 0$ and $dW/dX = 0$ and at X = 1, W = 1.0. As the coupled equations cannot be solved analytically, a finite difference approach is adopted. Eqns.(11), (12) and (13) in finite difference form become respectively

$$\frac{T^*_{i+1} - T^*}{\Delta X} = \frac{1}{2}\left(\mu W_i \frac{w_L}{L} + 2\right) \tag{14}$$

$$-T^*_i \left\{\frac{W_{i-1} - 2W_i + W_{i+1}}{\Delta X^2}\right\} + \frac{\mu W_i}{\tan\phi_r} = 0 \tag{15}$$

$$P^* = \mu W_L \frac{1}{n}\left[\frac{W_1 + 1}{2} + \sum_{i=2}^{n} W_i\right] \tag{16}$$

where $\Delta X = 1/n$

n = the number of sub-elements in to which the reinforcement strip is divided into,

W_i = normalised displacement at node 'i'.

T^*_i = normalised tension at node 'i'.

Solving for normalised displacement and normalized tension, one gets

$$W_i = \frac{T_i^* n^2 \left(W_{i-1} + W_{i+1}\right)}{\left(2n^2 T_i^* + \dfrac{\mu}{2\tan\phi_r}\right)} \tag{17}$$

$$T_{i+1}^* = \frac{1}{2n}\left\{\mu W_L W_i + 2\right\} + T_i^* \tag{18}$$

Location of Active Length of Reinforcement and Solution

The active length of reinforcement, x_o, is obtained by equating the reinforcement length associated with change in geometry to the increased length compatible with the strains associated with the developed tensile stresses along the reinforcement (Burd, 1995). Thus the increased length of the portion of reinforcement, A^1B, due to tensile stresses along the reinforcement should equal the length between A^1-B^1 obtained from the change in geometry of the portion, A^1B due to the application of downward displacement/force (Fig.4). To locate the position of A^1, the reinforcement length is discretized into 'n' elements [1, 2, 3, ..., (n+1) nodes]. The position of A^1 is located by traversing from $(n+1)^{th}$ node towards node 1. As there is no shear stress mobilized to the left of A^1, the tension developed at all nodes to the left of and at A^1 is zero. Supposing that A^1 corresponds to some node $j\left(1 \le j \le n+1\right)$, the extended length, L_e^1, of reinforcement between A^1-B, calculated from the reinforcement strains is

$$L_e^1 = x_o + \int_{L-x_o}^{L} \frac{T(x)}{J}\,dx \tag{19}$$

where $T(x)$ is the tension developed in the reinforcement at distance x.

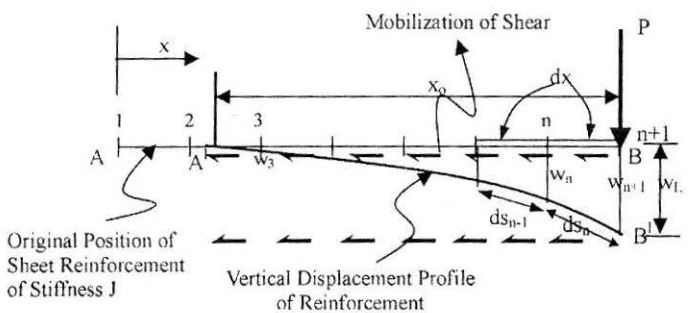

FIGURE 4 : Procedure for Calculation of Horizontal Displacements along the Reinforcement

In finite difference form, the above equation becomes

$$L_{\ell}^{1} = x_o + \sum_{i=j}^{n} \frac{T_i(x)}{J} dx_i \tag{20}$$

where x_o = unstretched length of A^1B,

J = modulus of deformation of the reinforcement and

$T_i(x)$ = average tension developed in the i^{th} element.

The length of reinforcement, L_g^1, between A^1-B, calculated from the change in geometry due to enforced transverse displacement/force at point B, is given by

$$L_g^1 = \int_{L-x_o}^{L} \sqrt{1+\left(\frac{dw}{dx}\right)^2}\, dx \tag{21}$$

In finite difference form, Eqn.(21) becomes

$$L_g^1 = \sum_{i=j}^{n} \sqrt{1+\left(\frac{\Delta w_i}{\Delta x_i}\right)^2}\, dx_i \tag{22}$$

Eqns.(20) and (22) after normalizing reduce to

$$L_{\ell}^{1\,*} = X_o + \sum_{i=j}^{n} \frac{T_i^*(x)}{J^*} \sqrt{\left(\frac{w_L}{L}\right)^2 (w_{i+1}-w_i)^2 + \left(\frac{1}{n-1}\right)^2} \tag{23}$$

$$L_g^{1\,*} = \sum_{i=j}^{n} \sqrt{\left(\frac{w_L}{L}\right)^2 (w_{i+1}-w_i)^2 + \left(\frac{1}{n-1}\right)^2} \tag{24}$$

where $L_{\ell}^{1\,*} = L_{\ell}^1/L$,

$L_g^{1\,*} = L_g^1/L$,

$X_o = x_o/L$,

$T^* = T/T_{max\,ap}$,

$T_{maxap} = 2\gamma D_e L \tan\phi_r$, the maximum axial pullout force and

$J^* = J/2\gamma D_e L \tan\phi_r$, the relative stiffness factor of the reinforcement.

X_o is to be located iteratively. Suppose in the process of node traversing to locate X_o, one is at node 'k', the boundary conditions to solve the governing equations for a given model are: the tension developed in the reinforcement at and all nodes to the left of 'k' are zero, i.e. $T_i = 0.0$, for $1 \le i \le k$ and the slope at node 'k' is zero, i.e., $(dw/dx)_i$ $\left[\text{or } (dW/dX)_i\right]$ $= 0$ at i = k. while at the right end, i.e. at x = L or X = 1.0, the displacement $w = w_L$ (or W = 1.0).

Using the above boundary conditions, the governing Eqns.(17) and (18) for the model are solved iteratively for normalized displacements and normalized tensions in the geosynthetics for the given relative stiffness and normalized front end displacement at the right of the reinforcement. $L_r^{!*}$ and $L_g^{!*}$ are evaluated from Eqns.(23) and (24) and equated. In case they are unequal, another immediate node to the left of node k, i.e. (k−1) is selected and the above procedure repeated. This process of node traversing is continued until the absolute differences $\left(L_r^{!*} - L_g^{!*}\right)$ at i^{th} node, i.e. $\left|\left(L_r^{!*} - L_g^{!*}\right)_i\right|$ and at $(i+1)^{th}$ node, i.e. $\left|\left(L_r^{!*} - L_g^{!*}\right)_{i+1}\right|$ computed using Eqns.(23) and (24) are equal. To start with, k is taken to be at node (n+1) and 'k' is traversed from node (n+1) towards 1. The maximum value of X_o can be 1.0 i.e. $x_o = L$, the full length of reinforcement (the case in which the shear stresses are mobilized over the entire length of the reinforcement).

The normalized displacements and tensions for this active length of the reinforcement are the actual displacements and tensions. The normalized transverse force, P^*, is then obtained from Eqn.(16).

The reinforcement is divided into 1000 elements and as the slope of the reinforcement, θ, is considered to be small, the normalized front end displacement, W_L, is restricted to a maximum value 0.01. Parametric studies have been carried out for w_L/L = 0.001 to 0.01; D_e = 1 to 10 m; L = 2

TABLE 1 : Modulus of Subgrade Reaction in MN/m³

Soil Characteristics	Loose	Medium Dense	Dense
Dry or Moist Sand	6-18	18-90	90-300
Submerged Sand	7.5	24	90

to 8 m; ϕ_r = 20° to 40°, γ = 15 to 20 kN/m^3 and J = 0 to 10,000 kN/m. The values of coefficient of subgrade reaction, k_s, considered (Scott, 1981) are shown in Table 1. For the above ranges of parameters, the relative subgrade stiffness factor, μ (= $k_s L/\gamma D_e$) ranges between 50 - 100,000 and relative stiffness factor for reinforcement, J^*, ranges from 0 - 1,000.

Results

A parametric study is carried out for quantifying the normalized values of the active length of reinforcement, X_o, the displacement, W^*(= w/L), the tension, T^*, the transverse force, P^*, maximum tension at right end, T^*_{max}, slope or inclination of reinforcement at right end, θ_L, and the normalized pullout force, $T^*_{max}\cos\theta_L$.

Relatively Softer Subgrades/Fills

Low value of μ (= $k_s L/\gamma D_e$) indicate relatively soft subgrades or deeper depths of embedment of reinforcement. Hence to simulate a relatively softer subgrades, a low value of μ = 500 is considered to study the effect of relative stiffness factor, J^*, in this type of subgrades/fills.

Variation of Active Length of Reinforcement, X_o with W_L

For a given relative stiffness of reinforcement, J^*, the normalized active length of reinforcement, X_o, increases with increase in front end displacement, W_L (Fig.5). Only a very small part of the reinforcement gets elongated (i.e.

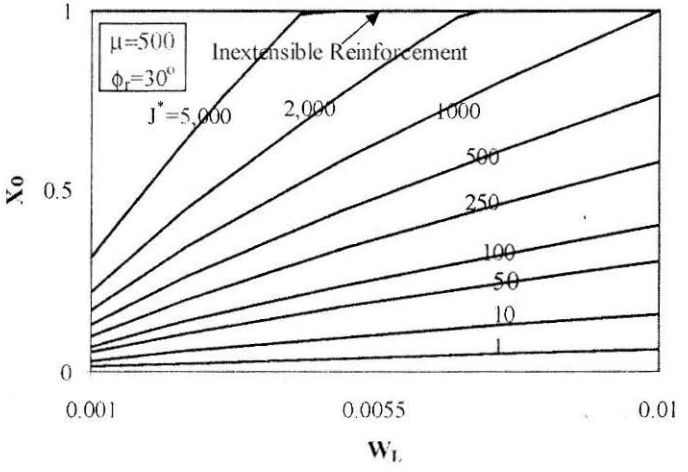

FIGURE 5 : Normalised Active Length of Reinforcement, X_o, Vs. W_L for Relatively Soft Subgrades (μ = 500) – Effect of J^*

$X_o < 1.0$) for reinforcements with low J^* values (≤ 1000). Full length of reinforcement gets stretched and hence the shear stresses are mobilised over the full length of reinforcement beyond certain front end displacement, W_L, for large J^* (≥ 1000). X_o becomes equal to 1.0 even at very small front end displacements, W_L, for these J^* values. $X_o = 1.0$ at $W_L = 0.005$ and 0.0075 for $J^* = 5000$ and 2000 respectively for $\mu = 500$ and $\phi_r = 30°$.

Displacement and Tension Profiles

The length over which the reinforcement undergoes transverse deformations increases with increase in relative stiffness factor, J^*. The normalized transverse displacements, W^*, are zero or negligibly small for $X < 0.76$ and increase sharply to 1.0 beyond $X = 0.76$ for $\mu = 500$ and $\phi_r = 30°$ and at a front end displacement of $W_L = 0.01$ (Fig.6). The reinforcement undergoes transverse displacements, W^*, only over a small length, $0.96 < X < 1.0$, for relatively highly extensible reinforcements ($J^* = 1.0$) whereas this zone increases to $0.79 < X < 1.0$ for relatively stiff reinforcements ($J^* \geq 1000$). The transverse displacement profile for $J^* \geq 1000$ is identical to that of an inextensible reinforcement (Madhav and Umashankar, 2002)

The variations of normalized tension with normalized distance for relative stiffness of the reinforcement, $J^* = 1$, 10, 50, 100, 250, 500 and ≥ 1000 for $w_L/L = 0.01$, $\mu = 500$ and $\phi_r = 30°$, are depicted in Fig.7. As the reinforcement stiffness increases, large tracts of reinforcement-soil interfaces mobilize shear resistance. For $J^* = 1$, shear resistance is mobilized only over a length of 0.1L from the right end whereas for $J^* \geq 1000$, shear

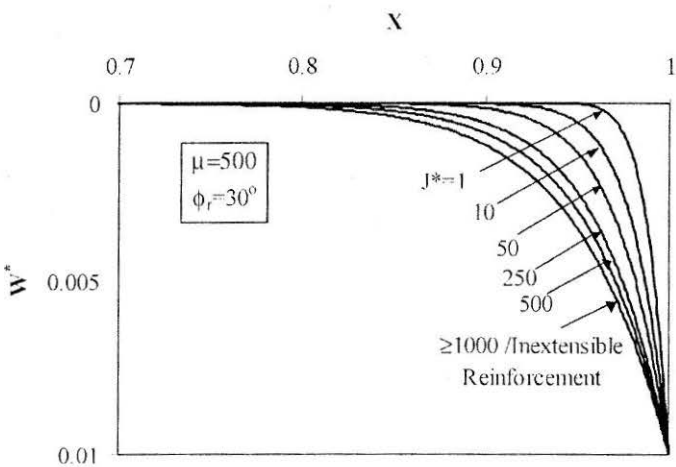

FIGURE 6 : Effect of J^* on Transverse Displacement Profiles for Relatively Soft/Weak Subgrades ($\mu = 500$)

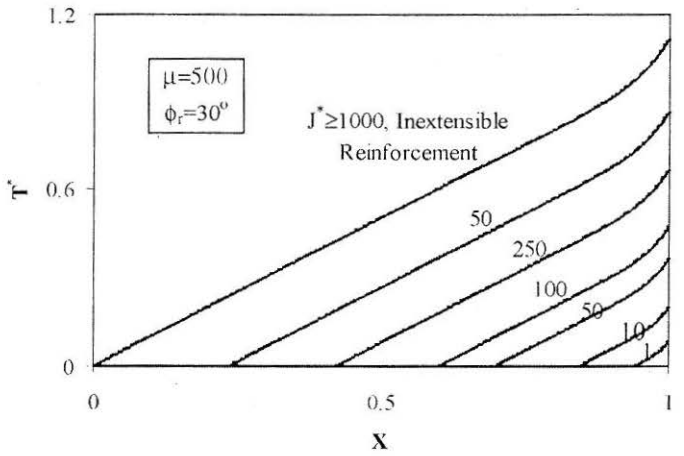

FIGURE 7 : Effect of J^* on Tension Profiles for Relatively Soft/Weak Subgrades (μ = 500)

resistance is mobilized over the entire length of reinforcement for μ = 500 and ϕ_r = 30° and at a front end displacement, W_L = 0.01. For a given relative stiffness of the reinforcement, the tension increases linearly over the initial portion of the reinforcement. The variation of tension with distance becomes non-linear near the right end of the reinforcement where large transverse displacements are mobilised. The mobilization of transverse displacements causes an increase in the shear resistance along the interface. The normalized tension profile for $J^* \geq 1000$ is identical to that of an inextensible reinforcement (Madhav and Umashankar, 2002)

Variations of P^*, T^*_{max}, θ_L and $T^*_{max} \cos\theta_L$ with W_L

The normalized transverse force, P^*, increases almost linearly with front end displacement, W_L, for relatively extensible reinforcements ($J^* \leq 50$). The increase of P^* with W_L is non-linear for increasing relative stiffness values of reinforcement (Fig.8). Very small normalized transverse force is sufficient to cause a given front end displacement for highly extensible reinforcement as the length over which the shear resistance gets mobilized is small. P^* = 0.05 is sufficient to give W_L = 0.01 for J^* = 1.0 and for μ = 500 and ϕ_r = 30°. But for relatively large relative stiffness of reinforcement (J^* = 1000), P^* value as high as 0.24 is required to cause the same displacement as the shear resistance is mobilized almost over entire length for the same set of parameters. The variation of P^* with W_L becomes identical to that of inextensible reinforcement for $W_L \geq 0.007$ for J^* = 2000 and for $W_L \geq 0.004$ for J^* = 5000 for the above set of parameters (Madhav and Umashankar, 2002)

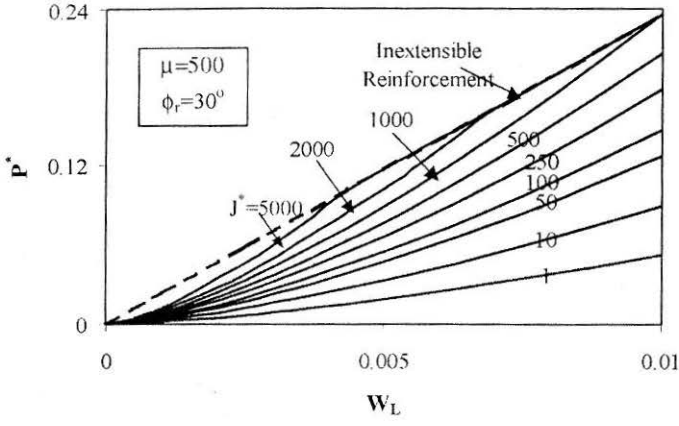

FIGURE 8 : Normalised Transverse Force, P^*, Vs. W_L for Relatively Soft Subgrades (μ = 500) – Effect of J^*

The maximum tension developed, T^*_{max} in the reinforcement at x = L is almost negligible for highly extensible reinforcements (J^* = 1.0) as the shear resistance is mobilized over small tracts of reinforcement. T^*_{max} varies almost linearly with W_L in the entire range 0.001 to 0.01 for J^* varying from 1.0 to 1000 (Fig.9). The tension developed at x = L is as low as 0.08 for J^* = 1.0 whereas it is as high as 1.12 for J^* = 1000 at W_L = 0.01 and for μ = 500 and ϕ_r = 30°. The variation of T^*_{max} with W_L for $W_L \geq 0.01$ for J^* = 1000, $W_L \geq 0.007$ for J^* = 2000 and $W_L \geq 0.004$ for J^* = 5000

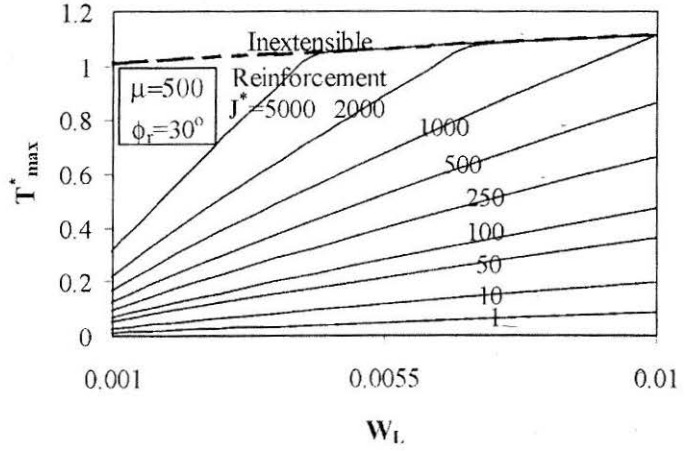

FIGURE 9 : Normalised Maximum Tension, T^*_{max}, Vs. W_L for Relatively Soft Subgrades (μ = 500) – Effect of J^*

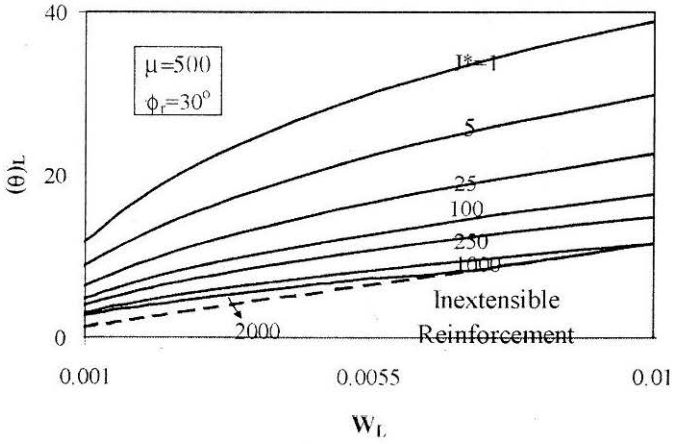

FIGURE 10 : Inclination of Reinforcement, θ_L, at X = 1 Vs. W_L for Relatively Soft Subgrades (μ = 500) – Effect of J^*

becomes identical to that for an inextensible reinforcement for μ = 500 and ϕ_r = 30°. T^*_{max} values predicted considering the reinforcement to be inextensible are considerably larger than those for extensible reinforcements.

The normal displacements are confined to a small portion near the right end for highly extensible reinforcements for a given free end displacement at the right end (Fig.6). Hence, the inclinations, θ_L, of highly extensible reinforcements with the horizontal at x = L are quite high. The inclination, θ_L, of reinforcement with relative stiffness, J^* = 1, is as high as 38° at x = L whereas it is 11.5° for J^* = 1000 and for W_L = 0.01, μ = 500 and ϕ_r = 30° (Fig.10). θ_L increases gradually with W_L. For J^* equal to 2000, the maximum inclination of the reinforcement, θ_L, for front end displacement, $W_L \geq 0.005$, becomes equal to that for an inextensible reinforcement for the above set of parameters.

The trend of variation of normalized axial component of pullout force, $T^*_{max}\cos\theta_L$, with normalised front end displacement, W_L, (Fig.11) is similar to that of the variation of normalized maximum tension, T^*_{max}, with W_L (Fig.9). The pullout force, $T^*_{max}\cos\theta_L$, is significantly less that the axial poullout capacity for highly extensible reinforcements ($J^* \leq 500$). But $T^*_{max}\cos\theta_L$ becomes larger than $T^*_{max\,ap}$ for relatively large stiffness of reinforcement and beyond certain front end displacements. $T_{max}\cos\theta_L > T_{max\,ap}$ for W_L greater than 0.0065 and 0.004 for J^* equal to 2000 and 5000 respectively for μ = 500 and ϕ_r = 30°. Thus the axial component of pull out force due to transverse displacement is marginally higher than the axial pull out capacity conventionally assumed in design for stiff reinforcement and transverse displacements, w_L, of the order of 0.05 or

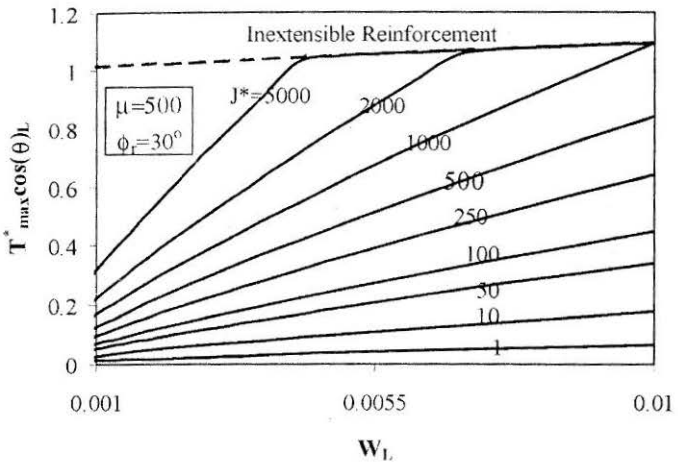

FIGURE 11 : Normalised Maximum Pullout Force, $T^*_{max}\cos\theta_L$, Vs. W_L for Relatively Soft Subgrades (μ = 500) – Effect of J^*

more. For all other cases, the axial capacity of pull out force due to transverse displacement could be considerably less than the axial capacity for extensible reinforcement in soft subgrades.

Relatively Stiffer Subgrades/Fills

High values of μ (= $k_s L/\gamma D_c$) indicate relatively stiff subgrades or shallow depths of embedment of reinforcement. Hence to simulate a relatively

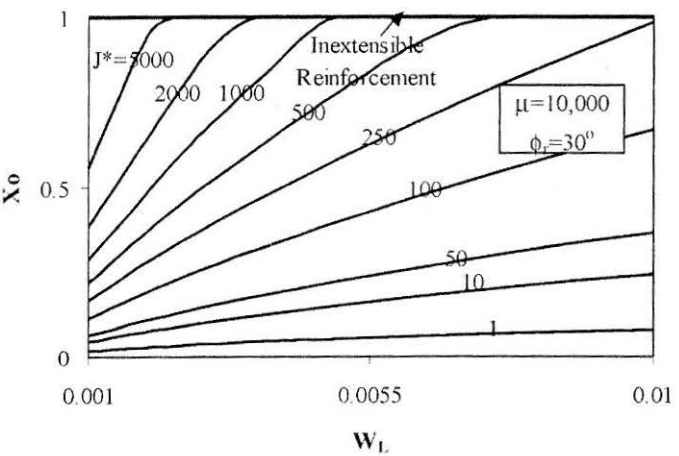

FIGURE 12 : Normalised Active Length of Reinforcement, X_o, Vs. W_L for Relatively Stiff Subgrades (μ = 10,000) – Effect of J^*

stiffer subgrades, a high value of μ = 10,000 is considered to quantify the effect of relative stiffness factor, J^*, on the response of the reinforcement to transverse displacement.

Variation of Active Length of Reinforcement, X_o with W_L

The variation of X_o with W_L (Fig.12) for μ = 10,000 is similar to that for relatively soft sills/subgrades (Fig.5). But larger lengths of reinforcement get stretched in stiffer fills/subgrades for a given relative stiffness of reinforcement. X_o is as high as 0.99 for μ = 10,000 whereas it is just 0.58 for μ = 500 for a reinforcement of relative stiffness, J^*, equal to 250 and W_L = 0.01. The full length of reinforcement gets elongated at smaller front end displacements in stiff fills/subgrades, i.e., full length of reinforcement gets elongated for $W_L \geq 0.025$ and 0.05 for μ = 10,000 and μ = 500 respectively for J^* = 5000 and ϕ_r = 30°.

Displacement and Tension Profiles

The normalized displacements, W^*, get highly localized near the right end for relatively stiff soils (μ = 10,000) (Fig.13). The transverse displacements are zero or negligibly small for $X < 0.93$ but increase sharply to 1.0 beyond X = 0.93 for μ = 10,000, ϕ_r = 30° and W_L = 0.01. Relatively extensible reinforcements undergo transverse deformation over a negligibly small portion in stiff soils. The transverse deformations take place over $0.98 < X < 1.0$ for μ = 10,000, J^* = 1.0, ϕ_r = 30° and at a front end displacement of W_L = 0.01. A comparison of Figs.6 and 12 reveals that the phenomena of localization of transverse displacements is predominant in stiff

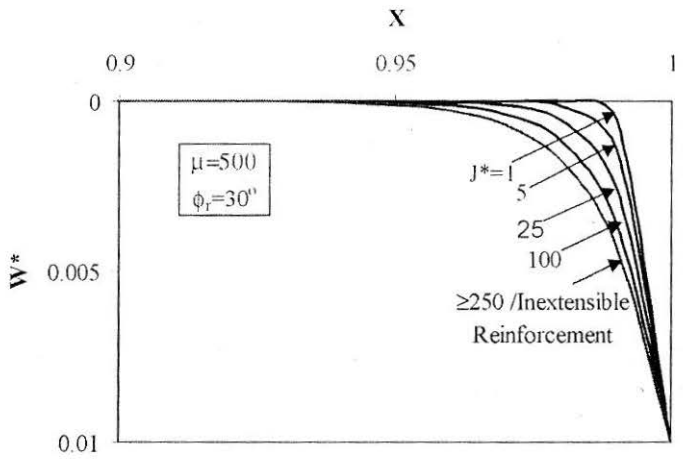

FIGURE 13 : Effect of J^* on Transverse Displacement Profiles for Relatively Stiff Subgrades (μ = 10,000)

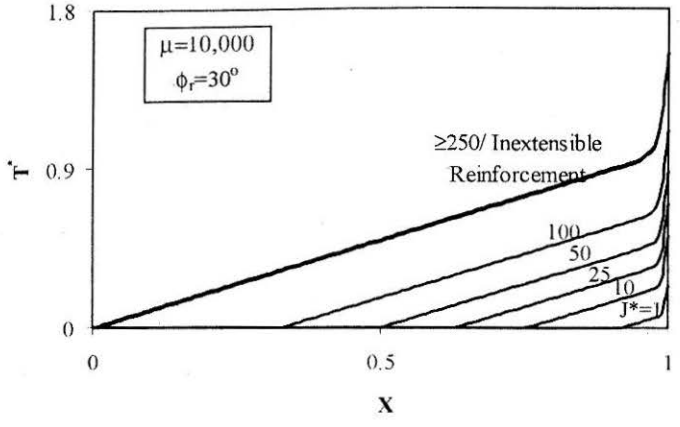

FIGURE 14 : Effect of J^* on Tension Profiles for Relatively Stiff Subgrades (μ = 10,000)

soils and the transverse displacements become identical to those for inextensible reinforcements even at smaller stiffness of reinforcement, J^*, in stiff soils. The transverse displacements are identical to inextensible reinforcements at a relative reinforcement stiffness, $J^* \geq 250$ in stiff soils (μ = 10,000) whereas the corresponding value is as high as $J^* \geq 1000$ for μ = 500 for ϕ_r = 30° and W_L = 0.01.

The variation of normalized tension, T^*, with normalized distance, X, for stiff fills/subgrades (μ = 10,000) (Fig.14) is similar to that for soft fills/ subgrades (μ = 500) (Fig.7). But the tension mobilized in the reinforcement is higher in stiffer fills/subgrades compared to the values in softer fills/ subgrades because of large stiffness of the subgrade and as the active length over which large shear stresses gets mobilized is higher for the former for a given relative stiffness, J^*, of reinforcement. The tension profiles for $J^* \geq 250$ become identical to that for an inextensible reinforcement for μ = 10,000 and ϕ_r = 30°.

Variations of P^*, T^*_{max}, θ_L and $T^*_{max}\cos\theta_L$ with W_L

The variation of normalized transverse force, P^*, with W_L (Fig.15) for reinforcement in stiff fills/subgrades (μ = 10,000) is similar to that of reinforcement in soft fills/subgrades (μ = 500) (Fig.8). P^* values are much higher for reinforcements in stiff fills/subgrades (μ = 10,000) compared to those for soft fills/subgrades (μ = 500). P^* value is 1.15 for μ = 10,000 compared to a value of 0.18 for μ = 500 for a relative stiffness of reinforcement, J^* = 250, for W_L = 0.01 and ϕ_r = 30°.

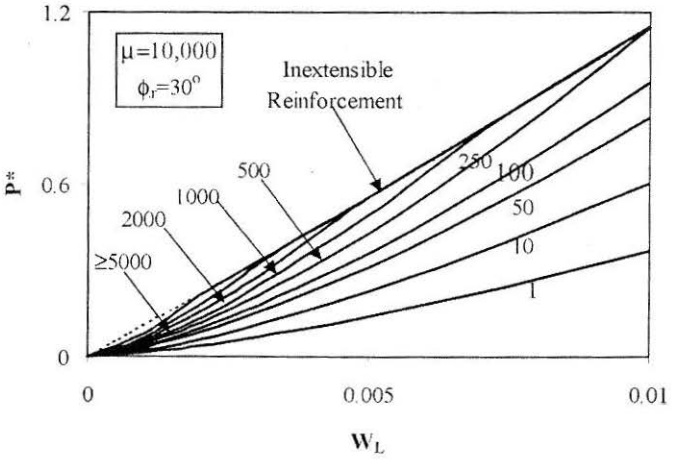

FIGURE 15 : Normalised Transverse Force, P^*, Vs. W_L for Relatively Stiff Subgrades (μ = 10,000) – Effect of J^*

The trends of variations of other quantities, viz., the maximum tension, T^*_{max}, the inclination, θ_L, of reinforcement at X = 1.0 and the maximum pullout force, $T^*_{max}\cos\theta_L$, with W_L for μ = 10,000, are found to be similar to those for μ = 500. But the magnitudes are significantly different. The axial pull out resistance, $T^*_{max}\cos\theta_L$, due to transverse displacement of the reinforcement is found (Fig.16) to be greater than the resistance, $T_{max\,ap}$, for W_L greater than 0.007, 0.006, 0.004, 0.003 and 0.002 for J^* equal to 250,

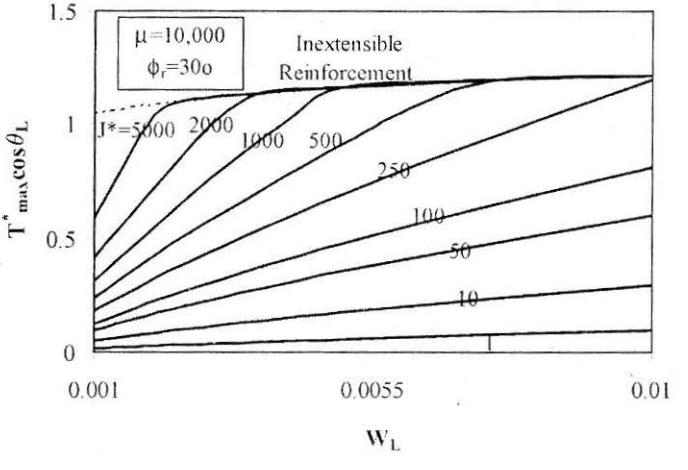

FIGURE 16 : Normalised Maximum Pullout Force, $T^*_{max}\cos\theta_L$ Vs. W_L for Relatively Stiff Subgrades (μ = 10,000) – Effect of J^*

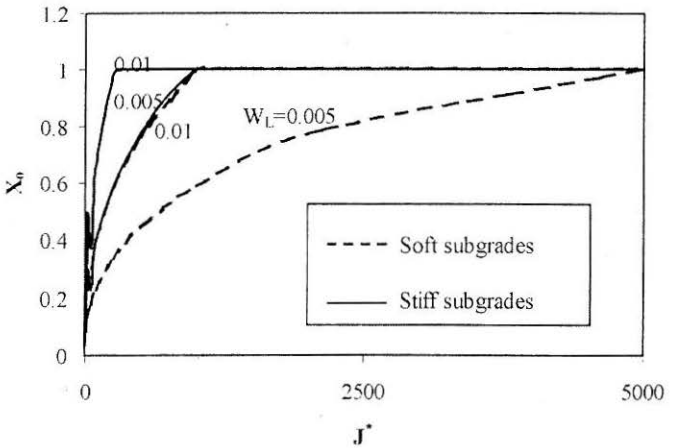

FIGURE 17 : Normalised Active Length of Reinforcement, X_o, Vs. J^* for Relatively Soft (μ = 500) and Stiff Subgrades (μ = 10,000) Subgrades – Effect of W_L

500, 1000, 2000 and 5000 respectively for μ = 10,000 and ϕ_r = 30°. Thus the axial component of pullout force due to transverse displacement is larger than the corresponding one for pure axial pull out.

Variations of X_o, P^*, T^*_{max}, θ_L and $T^*_{max}\cos\theta_L$ with J^*-Effect of W_L

The variation of X_o with J^* is depicted in Fig.17 for front end displacements of W_L, equal to 0.005 and 0.01 for soft and stiff fills/subgrades. The value of X_o increases continuously with J^*. The rate of increase of X_o with J^*, increases with both W_L and μ. Larger the values of W_L and μ, the faster is the increase of X_o with J^* indicating stiffer reinforcements gets elongated over larger lengths for these conditions. For a given stiffness and front end displacement, W_L, of reinforcement larger lengths of reinforcement get stretched (i.e. larger X_o values) for stiff fills/subgrades. Full length of reinforcement gets elongated (i.e. X_o = 1.0) for J^* values of 5000 and 2000 in softer fills/subgrades (μ = 500) and for J^* = 2000 and 500 for stiffer fills/subgrades (μ = 10,000) at front displacements, W_L, equal to 0.005 and 0.01 respectively and for ϕ_r = 30°.

The normalized transverse force, P^*, increases initially with the relative stiffness of reinforcement, J^*, and reaches a constant value (Fig.18). Thus the transverse force required to cause a given front end displacement is independent of J^* beyond a certain value of J^*. P^* is 1.15 for $J^* > 500$ and μ = 10,000 whereas it is 0.24 for $J^* > 1000$ μ = 500 at a front end displacement, W_L, equal to 0.01, and ϕ_r = 30°.

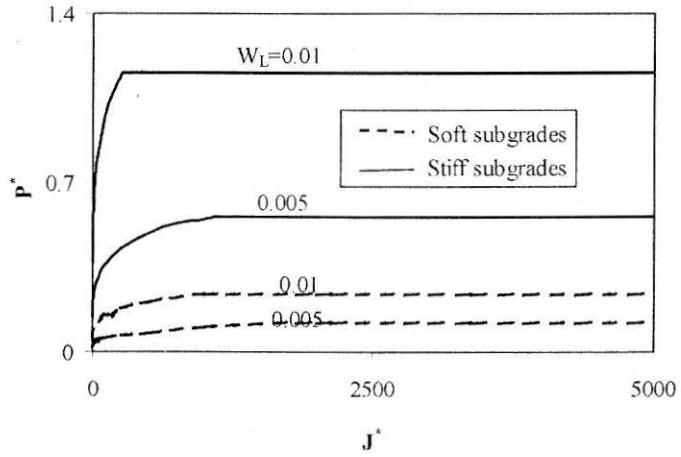

FIGURE 18 : Normalised Transverse Force, P^*, Vs. J^* for Relatively Soft (μ = 500) and Stiff Subgrades (μ = 10,000) Subgrades – Effect of W_L

The variations of maximum normalized tension developed, T^*_{max}, (Fig.19) in the reinforcement at x = L with J^* are very similar to the trends exhibited by the variations of active length of reinforcement, X_o, with J^* (Fig.17).

The transverse displacements, W^*, become highly localized near the right end of reinforcement for very stiff fills/subgrades and for highly

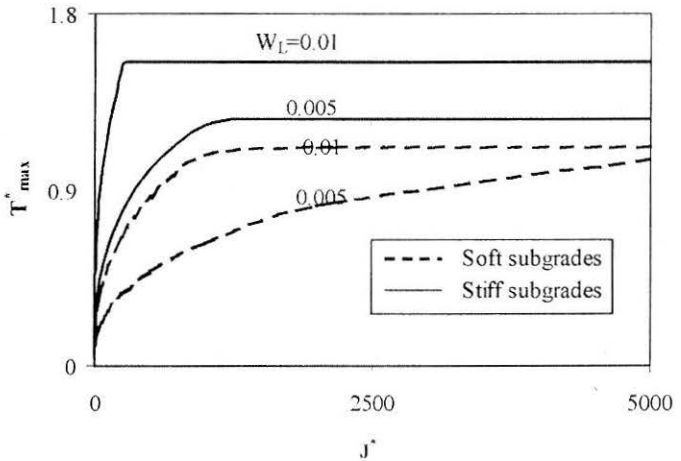

FIGURE 19 : Normalised Maximum Tension, T^*_{max}, Vs. J^* for Relatively Soft (μ = 500) and Stiff Subgrades (μ = 10,000) Subgrades – Effect of W_L

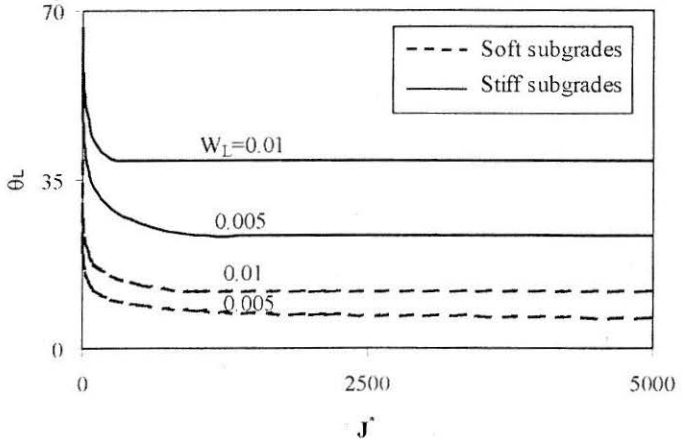

FIGURE 20 : Inclination of Reinforcement, q_L at X = 1 Vs. J^* for Relatively – Effect of W_L

extensible reinforcements (Fig.13). The transverse deformations remain constant beyond certain relative stiffness of reinforcement. Hence, the inclination of reinforcement, θ_L, at x = L decreases initially with increase in the relative stiffness of reinforcement, J^*, but remains constant beyond certain stiffness of reinforcement (Fig.20). The inclination is high at about 39° for $J^* \geq 500$ and $\mu = 10{,}000$ but is just 11° for $J^* \geq 1000$ and $\mu = 500$ for front end displacement, $W_L = 0.01$, and $\phi_r = 30°$.

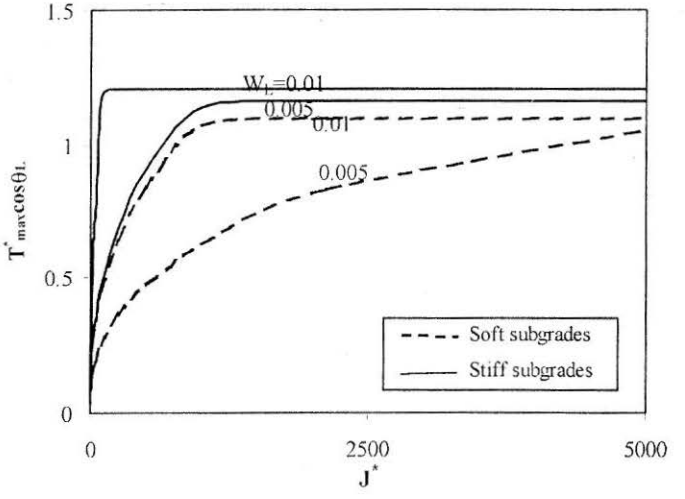

FIGURE 21 : Normalised Maximum Pullout Force, $T^*_{max} \cos\theta_L$, Vs. J^* for Relatively Soft (μ = 500) and Stiff Subgrades (μ = 10,000) Subgrades – Effect of W_L

The variation of normalized axial component of pullout force, $T^*_{max}\cos\theta_L$, developed in the reinforcement at x = L with J^* (Fig.21) is similar to the variation of maximum normalized tension developed, T^*_{max}, in the reinforcement at x = L with J^* (Fig.19). $T^*_{max}\cos\theta_L$ is more than the axial pullout capacity by 21% for $J^* \geq 100$ and μ = 10,000 and 9% for $J^* \geq 1000$ and for μ = 500 for a W_L = 0.01 and ϕ_r = 30°.

Variation of Transverse Pull and Axial Pullout for Typical Fill/Subgrade Properties

The variation of transverse pull and axial pullout at various transverse displacements for typical values of k_s = 20,000 kN/m^3, L = 3 m, D_e = 6 m, γ = 20 kN/m^3 and J = 5000 kN/m is presented in Table 2. The axial pullout capacity for a purely axial pull is 415.7 kN for the above subgrade and reinforcement properties whereas the axial pullout is quite less, depending on the transverse front end displacement, when inclination of the reinforcement is considered (Table 2).

Conclusions

The response of extensible reinforcement sheet embedded in a fill at depth and subjected to a transverse displacement is analysed by considering a linear subgrade response. The governing coupled equations are normalized and solved numerically. The variations of the several parameters such as transverse displacements and tension with distance, and of maximum tension, maximum inclination and the axial pullout capacity of reinforcement with normalized front end displacement as effected by the relative stiffness of reinforcement, J^*, are quantified. The study is carried for both soft/weak as well as stiff/strong subgrades/fills. A comparison is brought out in the responses of extensible and inextensible reinforcements to transverse pull/displacement. It is observed that the axial component of pullout force for

TABLE 2 : Variation of Transverse Force and Axial Pullout with Transverse Displacement (k_s = 20,000 kN/m^3, L = 3 m, D_e = 6 m, γ = 20 kN/m^3 and J = 5000 kN/m)

W_L (m)	P (kN)	$T_{max}\cos\theta$ (kN)
0.0015	0.418	7.232
0.0030	1.173	12.418
0.0075	4.518	26.010
0.0150	12.265	44.988
0.0225	22.014	62.332
0.0300	33.289	78.342

inextensible reinforcements is considerably higher than that for extensible reinforcements. The axial pullout for an inextensible reinforcment is nearly 90% greater when compared to a relatively extensible reinforcement with $J^* = 10.0$ for $W_L = 0.005$, $\mu = 500$ and $\phi_r = 30°$. Hence, it is very important to consider the extensibility of the reinforcement in the analysis.

The active length, $x_o = 0.09L$ for $J^* = 10.0$ whereas it is $1.00L$ for $J^* \geq 5000$ at $W_L \geq 0.005$, $\mu = 500$ and $\phi_r = 30°$. Thus, the active length of reinforcement increases with reinforcement stiffness and equals the full length of reinforcement for stiff reinforcements beyond a certain front end displacements. This front end displacement at which the full length of the reinforcement gets elongated decreases with increasing stiffnesses of the reinforcement and the subgrade. The axial component of pullout force remains nearly constant for $J^* \geq 5000$ for transverse front end displacement beyond $0.04L$ with fill/subgrade properties, $\mu = 500$ and $\phi_r = 30°$. The axial pullout is nearly 188% greater for a stiff fill/subgrade with $\mu = 10{,}000$ compared to a relatively soft fill/subgrade with $\mu = 50$ for a reinforcement with $J^* = 100.0$ and $\phi_r = 30°$. Thus, it is established that reinforcement subjected to transverse pull in stronger and stiffer granular fills offers a maximum pullout response that is significantly larger than the purely axial pullout capacity. This pullout response due to transverse displacement increases with the front end displacement, W_L, and with the stiffness of subgrade and reinforcement.

References

ALFARO, M.C., MIURA, N. and BERGADO, D.T. (1995) : "Soil-Geogrid Reinforcement Interaction by Pull Out and Direct Shear Tests", *Geotech. Testing J.*, ASTM, Vol.18, No.2, pp.157-167.

BERGADO, D.T. and LONG, P.V. (1997) : "Discussion Leader's Report: Embankments", In H. Ochiai, N. Yasufuku and K. Omine (Eds.) *Earth Reinforcement*, Vol.2, pp.1015-1022.

BURD, H.J. (1995) : "Analysis of Membrane Action in Reinforced Unpaved Roads", *Can. Geotech. J.*, Vol.32, pp.946-956.

BONAPARTE, R. and CHRISTOPHER, B.R. (1987) : "Design and Construction of Reinforced Embankments over Weak Foundation", *Trans. Res. Rec.*, No.1153, pp.26-39.

DELMAS, P., QUEYROI, D., QUARESMA, M., DE SAINT, AMAND and PUECH, A. (1992) : "Failure of an Experimental Embankment on Soft Soil Reinforced with Geotextile", *Guiche, Geomembranes and Related Products*, In: Den-hoedt, (Ed.), Balkema, Rotterdam.

FARRAG, K., ACAR, Y.B. and JURAN, I. (1993) : "Pull-out Resistance of Geogrid Reinforcements", *Geotext. and Geomem.*, Vol.12,133-159.

FOWLER, J. (1982) : " Theoretical Design Considerations for Fabric Reinforced Embankments", *Proc. 2nd Int. conf. on Geotextiles*, Vol.3, pp 665-670.

HAYASHI, S., MAKIUCHI, K. and OCHIAI, H. (1994) : "Testing Methods for Soil-Geosynthetic Frictional Behaviour – Japanese Standard, *Proc. 5th Int. Conf. on Geotextiles, Geomembranes and Related Products*, Vol.1, pp.411-414.

HUISMAN, M.G.H. (1987) : "Design Guideline for Reinforced Embankments on Soft Soils using Stabilenka Reinforcing Mats", *Enka Technical Report*, Anrheim.

INGOLD, T.S. (1983) : "Laboratory Pullout Testing of Grid Reinforcements in Sand", *Geotech. Test. J.*, Vol.6, No.3, pp.101-110.

JEWELL, R.A., MILIGAN, G.W.E., SARSBY, R.W. and DUBOIS, D. (1984) : "Interaction between Soil and Geogrids", *Proc. of the Symp. on Polymer Grid Reinf. in Civil Engrg.*, pp.19-29, Thomas Telford Limited, London, UK.

JEWELL, R.A. (1992) : Keynote Lecture : "Links Between the Testing, Modeling and Design of Reinforced Soil", *Proc. Int. Sym. on Earth Reinf. Practice*, Fukuoka, Japan, Vol.2, pp.755-772.

JEWELL, R.A. (1996) : "Soil reinforcement with geotextiles", *Publ. No.123*, CIRIA, 332p.

JURAN, I., KNOCHENNMUS, G., ACAR, Y.B. and ARMAN, A. (1988) : "Pullout Response of Geotextiles and Geogrids", *Geosyn. for Soil Improvement*, R.D.Holtz (ed.), Geotech. Spl. Publ., Vol.18, pp.92-111.

LESHCHINSKY, D. and BOEDEKER, R.H. (1989) : "Geosynthetic Reinforced Soil Structures", *J. Geotech. Engrg*, ASCE, Vol.115, No.10, pp.1459-1478.

LOPES, M.L. and LADEIRA, M. (1996) : "Role of Specimen Geometry, Soil Height and Sleeve Length on the Pull-O Behaviour of Geogrids", *Geosyn. Int.*, Vol.3, No.6, pp.701-719.

LOW, B.K. and DUNCAN, J.M. (1985) : "Analysis of the Behavior of Reinforced Embankments on Weak Foundation", *Report No.VPI/CE-GT-85-11*, Virginia Polytechnic Institute, Blacksburg, USA.

MADHAV, M.R. and UMASHANKAR, B (2003) : "Analysis of Inextensible Sheet Reinforcement subject to Transverse Displacement/Force: Linear Subgrade Response", *Geotext. & Geomem.*, Vol.21, No.2, pp 69-112.

McGOWN, A., ANDRAWES, K.Z. and KABIR, M.H. (1982) : "Load Extension Testing of Geotextiles confined in Soil", *Proc. 2nd Int. Conf. on Geotext.*, Vol.3, pp.793-796, Las Vegas.

OCHIAI, H., OTANI, J., HAYASHI, S. and HIRAI, T. (1996) : "The Pull-Out Resistance of Geogrids in Reinforced Soil", *Geotext. and Geomem.*, Vol.14, pp.19-42.

QUAST, P. (1983) : " Polyester Reinforcing Fabric Mats for the Improvement Embankment Stability", *Proc. 8th Int. Conf. on Soil Mech. and Found. Engrg.*, Vol.2, pp 531-534.

ROWE, K.R. and SODERMAN, K.L. (1984) : "Comparison of Predicted and Observed Behavior of Two Test Embankments", *Geotext. and Geomem.*, Vol.1, pp.157-174.

SCOTT, R.F., (1981) : *Foundation Analysis*, Prentice Hall Inc., Englewood Cliffs, New Jersey, 249 p.

SOBHI, S. and WU, J.T.H. (1996) : "An Interface Pull Out Formula for Extensible Sheet Reinforcement", *Geosyn. Int.*, Vol.3, No.5, pp.565-582.

TERZAGHI, K. (1955) : "Evaluation of Coefficient of Subgrade Reaction", *Geotechnique*, Vol.5, No.4, pp.197-226.

Notations

D_e = Embedment depth of reinforcement.

J = Stiffness of reinforcement.

J^* = Relative stiffness of reinforcement ($= J/T_{maxap}$, $T_{maxap} = 2\gamma D_e L \tan\phi_r$) .

k_s = Initial tangent modulus of subgrade reaction.

L = Length of reinforcement.

L_g^l = Extended length of reinforcement calculated from change in geometry.

L_g^{l*} = Extended length due to change in geometry normalized with length of reinforcement.

L_t^l = Extended length of reinforcement calculated from tensions along reinforcement.

L_t^{l*} = Extended length due to strains normalized with length of reinforcement.

n = Number of elements the reinforcement is divided.

P = Transverse force at front end.

P^* = Normalised transverse force ($= P/\gamma D_e L$).

q = Normal stress due to transverse displacement.

q_b = Stresses acting on bottom surface of reinforcement.

q_t = Stresses acting on top surface of reinforcement.

q_{ult} = Ultimate bearing resistance of the soil.

T = Tension developed in the reinforcement.

T_{maxap} = Axial pull out capacity ($= 2\gamma D_e L \tan\phi_r$).

T^* = Normalised tension developed in the reinforcement ($= T/T_{maxap}$, $T_{maxap} = 2\gamma D_e L \tan\phi_r$).

T^*_{max} = Normalised maximum tension in the reinforcement ($= T_{max}/T_{maxap}$)

w = Transverse displacement of reinforcement.

w_L = Transverse displacement at front end.

W = Transverse displacement of reinforcement normalized with w_L (= w/w_L).

W_L = Normalised front end displacement (= w_L/L).

W^* = Transverse displacement of reinforcement normalized with L (= w/L).

X = Normalized distance (= x/L).

x_o = Active length of reinforcement.

X_o = Active length normalized with length of reinforcement.

Δx = Length of infinitesimal element.

ΔX = Length of infinitesimal element in normalized form.

μ = Relative subgrade stiffness factor (= $k_s L/\gamma D_e$).

γ = Unit weight of soil.

ϕ_r = Interface angle of shearing resistance between reinforcement and soil.

θ = Inclination of reinforcement.

θ_L = Inclination/slope at front end.

τ = Mobilized shear stress at interface.

τ_b = Shear stresses on bottom surface of reinforcement.

τ_t = Shear stresses on top surface of reinforcement.

τ_{max} = Maximum shear stress that can be mobilized along interface.

$(\tau_{max})_b$ = Maximum shear stress that can be mobilized at bottom surface of reinforcement sheet

$(\tau_{max})_t$ = Maximum shear stress that can be mobilized at bottom surface of reinforcement sheet